Supplement of Atmos. Chem. Phys., 15, 4373–4387, 2015
http://www.atmos-chem-phys.net/15/4373/2015/
doi:10.5194/acp-15-4373-2015-supplement

Atmospheric Chemistry and Physics
Open Access

Supplement of

Near-highway aerosol and gas-phase measurements in a high-diesel environment

H. L. DeWitt et al.

Correspondence to: H. L. DeWitt (helen-langley.dewitt@univ-amu.fr) and N. Marchand (nicolas.marchand@univ-amu.fr)

Supplementary Graphs

1. Detailed Traffic Analysis

LDVs accounted for the majority of traffic (94%) and only experienced a small drop-off in flow over the weekends (87% of the weekday flow). HDVs and buses, however, were present in much higher concentrations during the week versus the weekend (2.7 times less buses and HDVs on the weekends), and also were in lower numbers on the road during the early morning and late evening hours. A relatively high correlation between the different Euro classifications of vehicles was observed (R^2 values of 0.7 for Euro 5 and Euro 4, 0.9 for Euro 3 and Euro 4, using 15 minute time resolution traffic data). For diesel cars, from Euro 4 (released in 2005) to Euro 5 (released in 2009), NOx emission limits decreased from 0.25 to 0.18 g km^{-1} and particulate emission limits decreased from 0.025 to 0.005 g km^{-1}. From Euro 3 (released in 2000) to Euro 4 another two-fold decrease in NOx and PM emission limits was implemented for diesel vehicles. Gasoline NOx emission limits were reduced from 0.15 to 0.08 to 0.06 g km^{-1} from Euro 3 to Euro 5, and total hydrocarbon emission limits were reduced from 0.20 to 0.10 g km^{-1} from Euro 3 to Euro 4. No PM limits were implemented for gasoline-powered vehicles until Euro 5, where a limit of 0.005 g km^{-1} for direct-injection vehicles was introduced, and no total hydrocarbon emission limits have been introduced for diesel-powered vehicles.

Figure S1: The number of diesel and gasoline vehicles per 15 minute (A). The number of bus, commercial vehicle (CV), and personal vehicle (PV) divided into Euro 0-5 categories (left axis, B) and the sum of Euro 0-5 for each category of vehicle (right axis, B). The colored squares correspond to four hour averages of vehicle concentrations (Euro 0-5).

b)

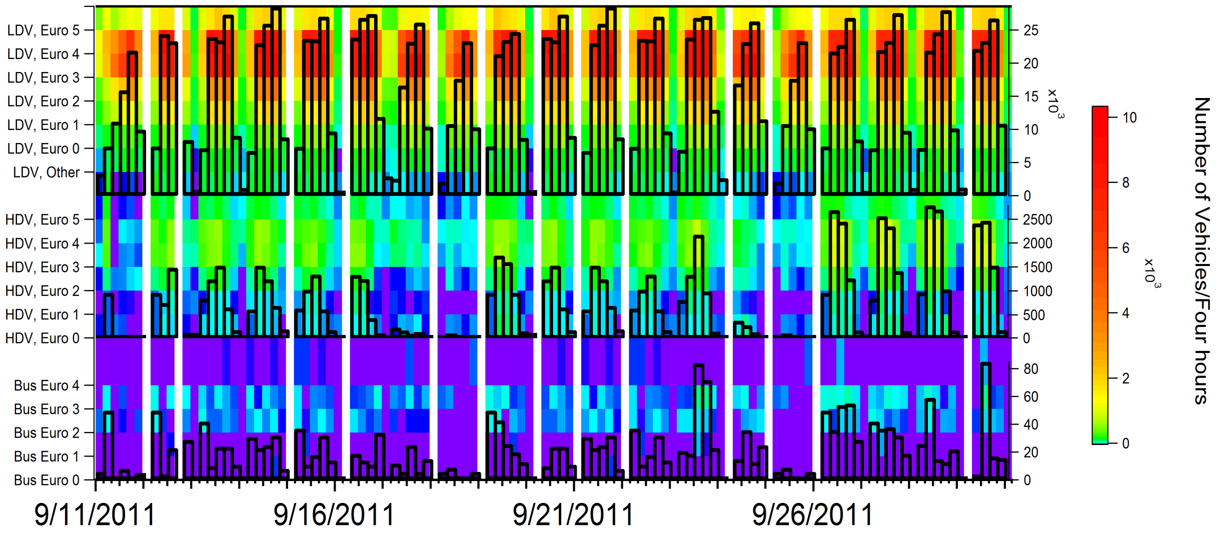

LDV, Euro 5
LDV, Euro 4
LDV, Euro 3
LDV, Euro 2
LDV, Euro 1
LDV, Euro 0
LDV, Other
HDV, Euro 5
HDV, Euro 4
HDV, Euro 3
HDV, Euro 2
HDV, Euro 1
HDV, Euro 0
Bus Euro 4
Bus Euro 3
Bus Euro 2
Bus Euro 1
Bus Euro 0
9/11/2011
9/16/2011
9/21/2011
9/26/2011
25
20
15
10
5
0
x10^3
2500
2000
1500
1000
500
0
80
60
40
20
0
10
8
6
4
2
0
x10^3
Number of Vehicles/Four hours

a)

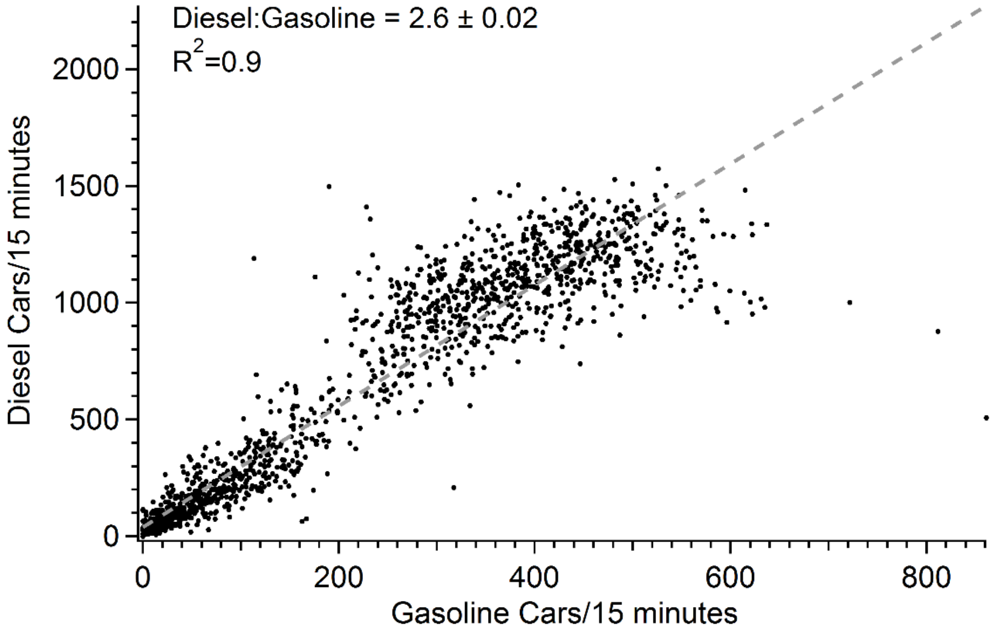

Diesel:Gasoline = 2.6 ± 0.02
R^2=0.9
2000
1500
1000
500
0
Diesel Cars/15 minutes
0
200
400
600
800
Gasoline Cars/15 minutes

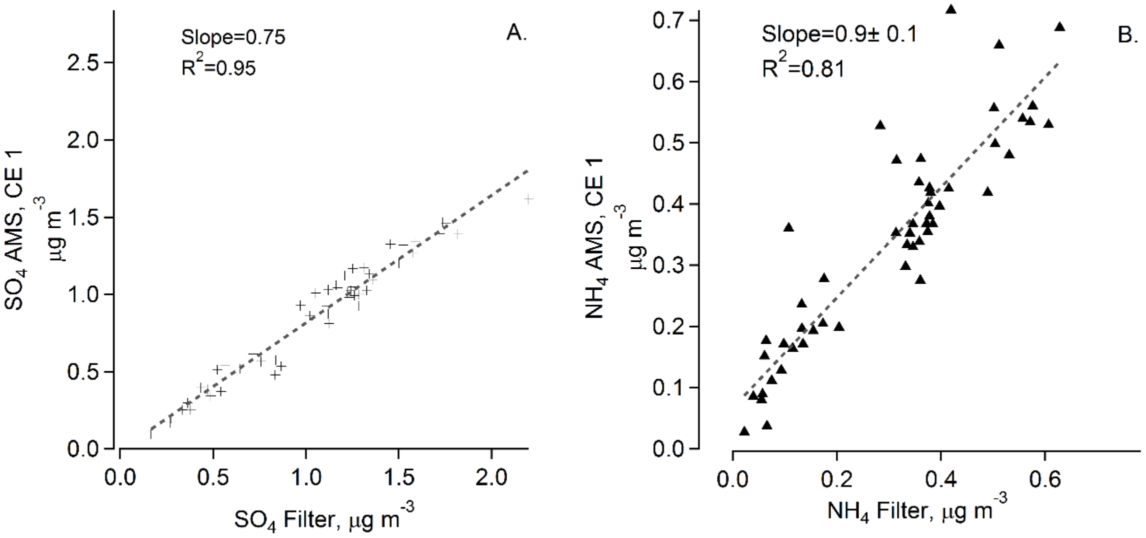

Figure S2: Comparison of filter data to uncorrected AMS data

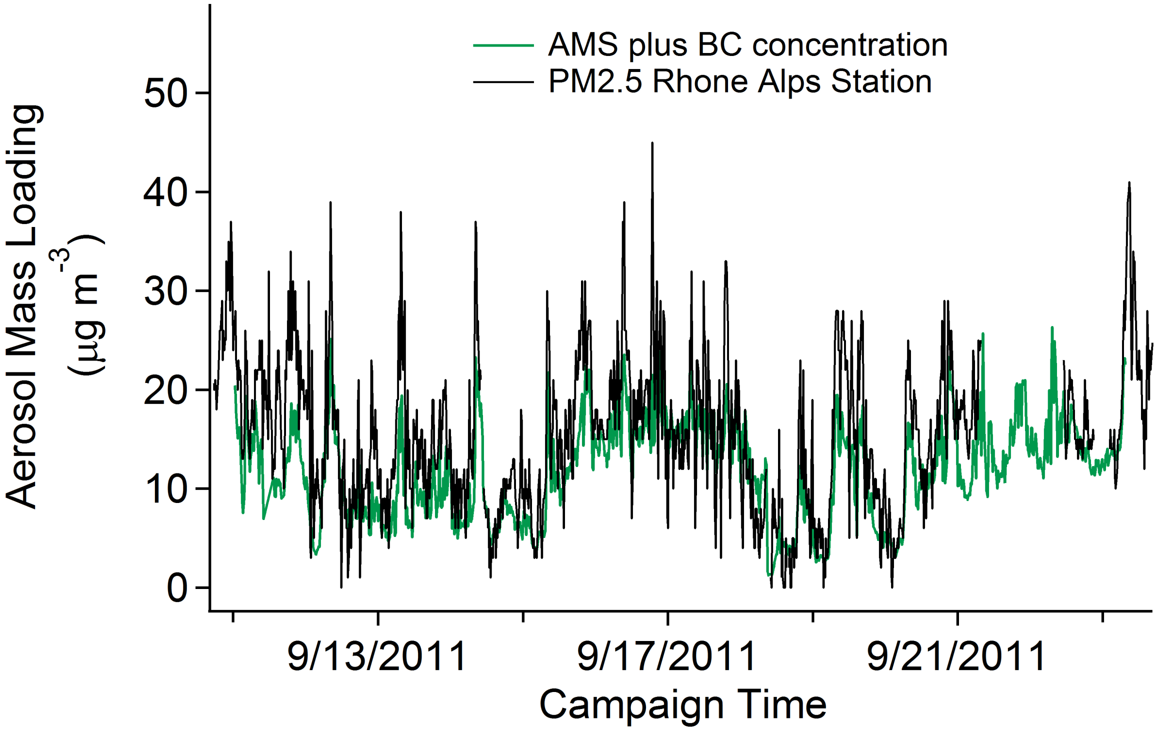

Figure S3: Rhone Alps PM2.5 data (black) time series compared to the AMS SO_4+NO_3+Org+NH_4 (CE=0.75) and MAAP BC data.

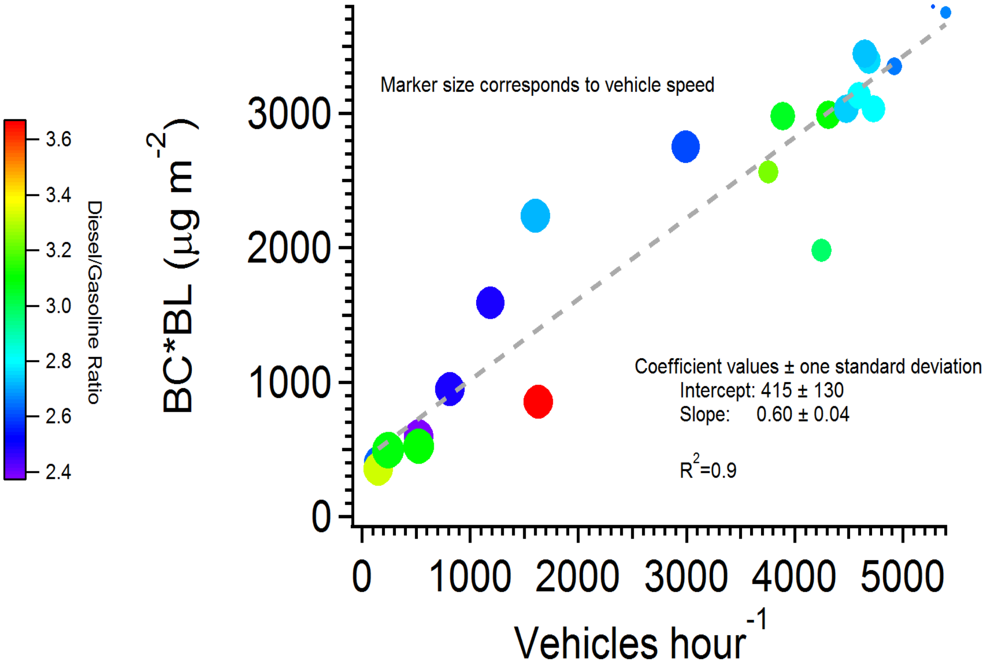

Figure S4: Diurnally averaged BC concentrations (multiplied by boundary layer height) versus diurnally averaged vehicle concentration. Colors correspond to diesel/gasoline ratio and the marker size corresponds to vehicle speed, from small (slow) to large (fast). Vehicle flux and BC negatively correlated with vehicle speed, indicating that both the number of vehicles and traffic flow (stop-and-go versus steady flow) likely influenced vehicular emissions.

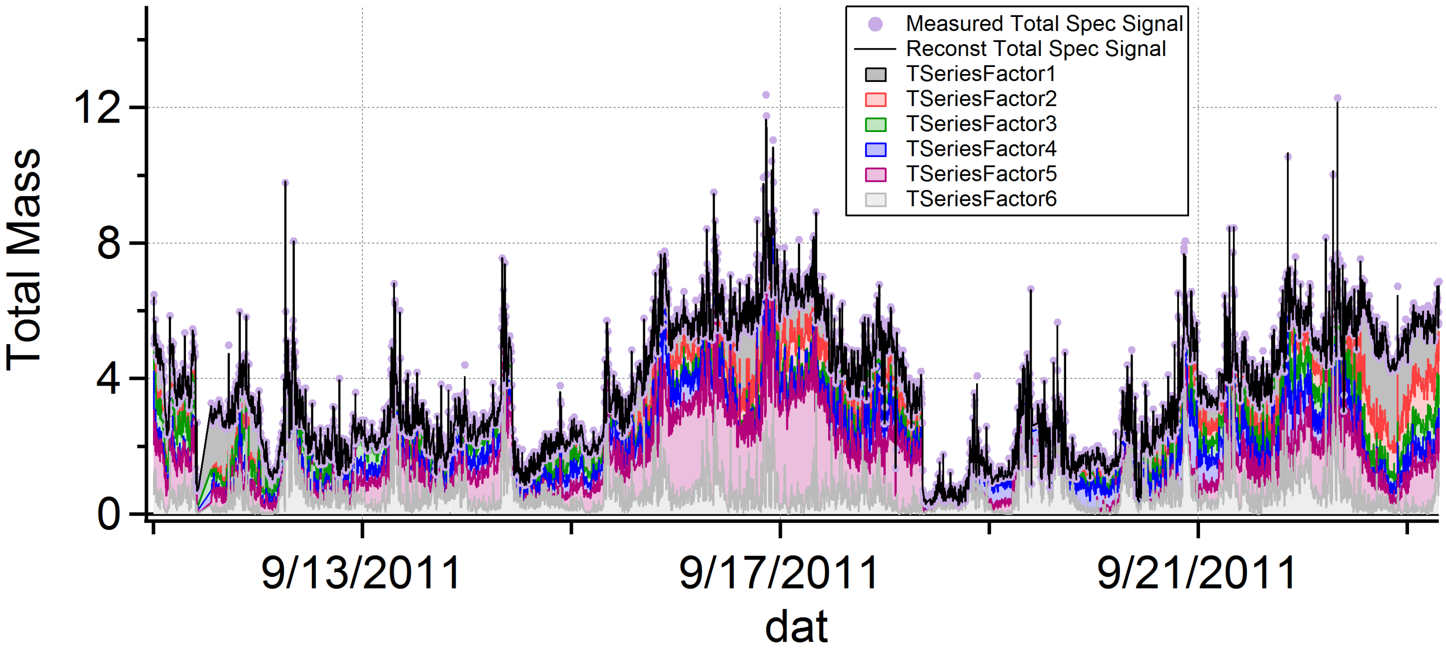

Figure S5:Tseries concentrations and total reconstructed signal for the six-factor PMF solution compared to the measured total signal (purple dots). Not CE corrected.

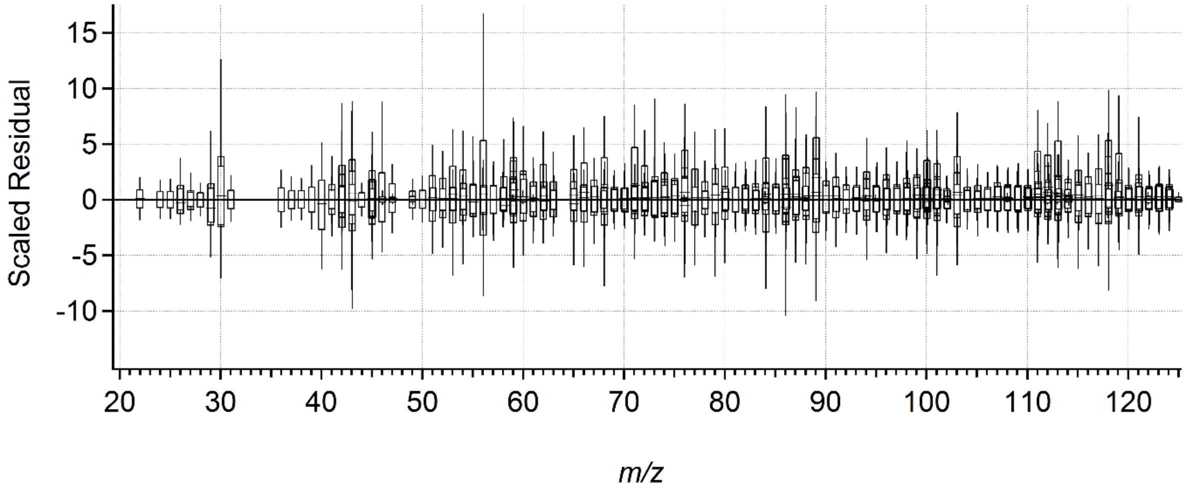

Figure S6: Scaled residuals for each high-resolution m/z input into the model for the six-factor PMF solution. Even distribution between positive and negative residuals.

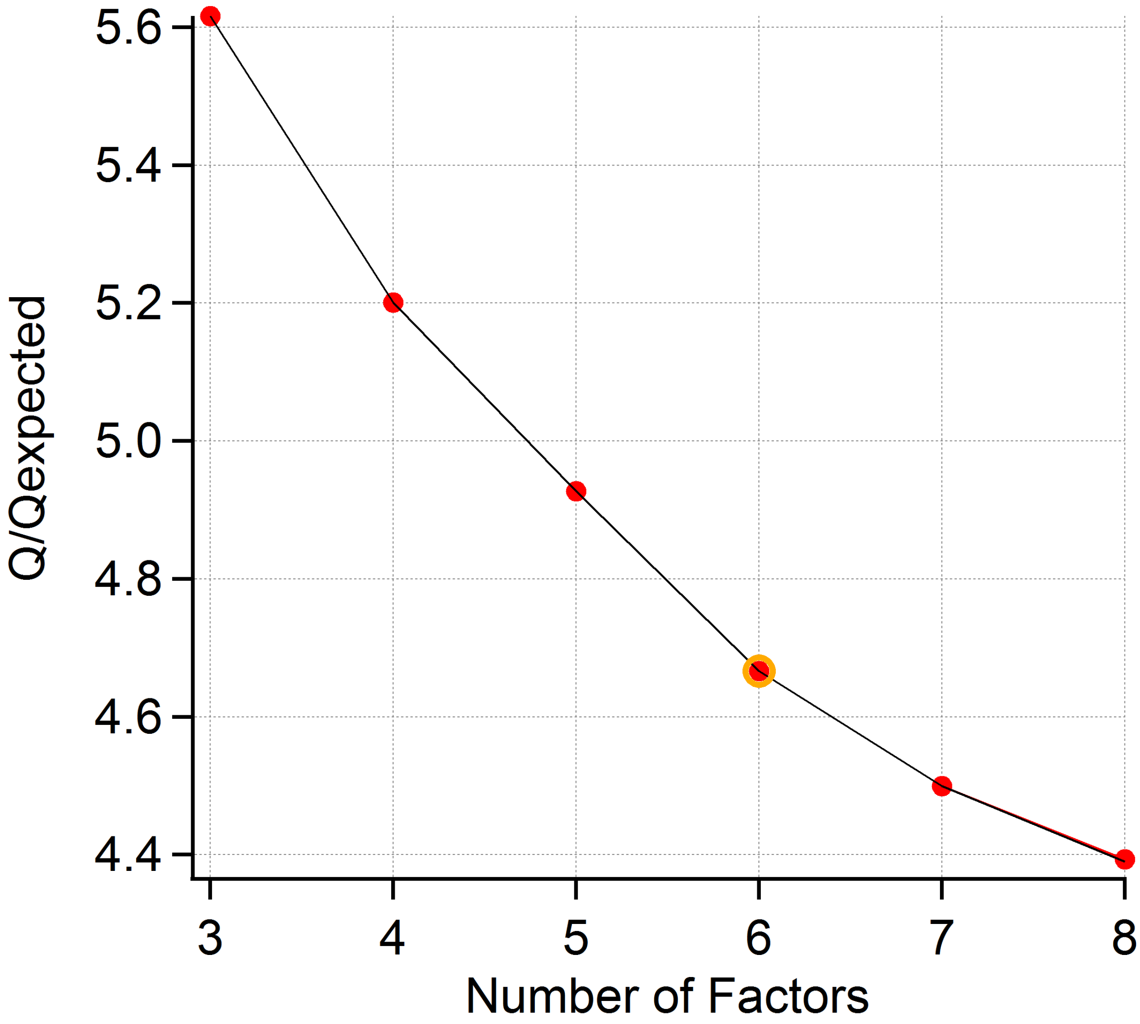

Figure S7: Q/Qexpected for 3-8 factor solutions.

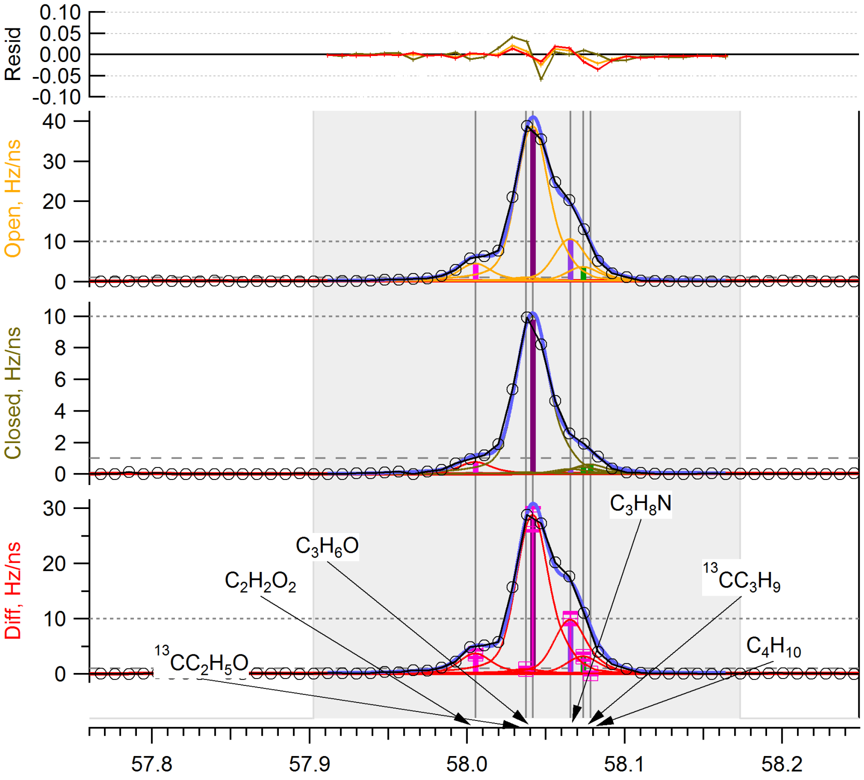

Figure S8: Nitrogen-containing organicpeak fitting.

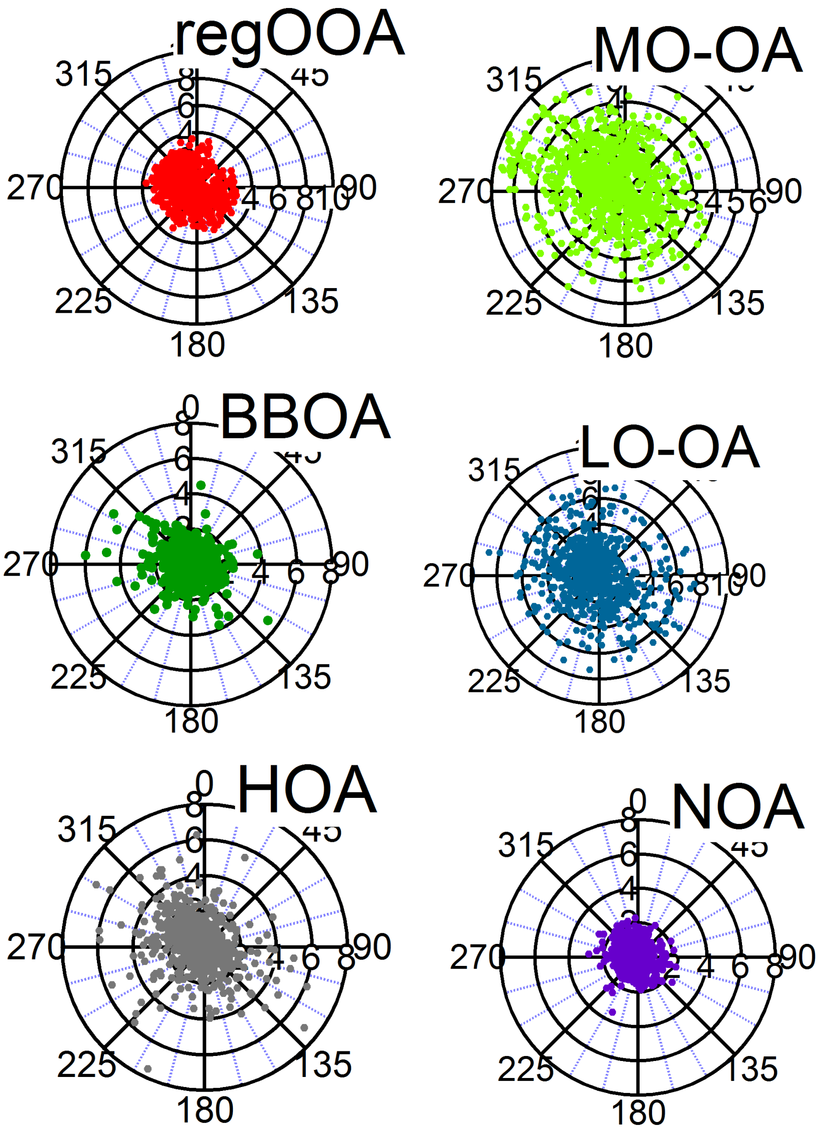

Figure S9: Polar graph plots of the six factor concentrations (radius, µg m^{-3}) and wind direction (angle, degrees).

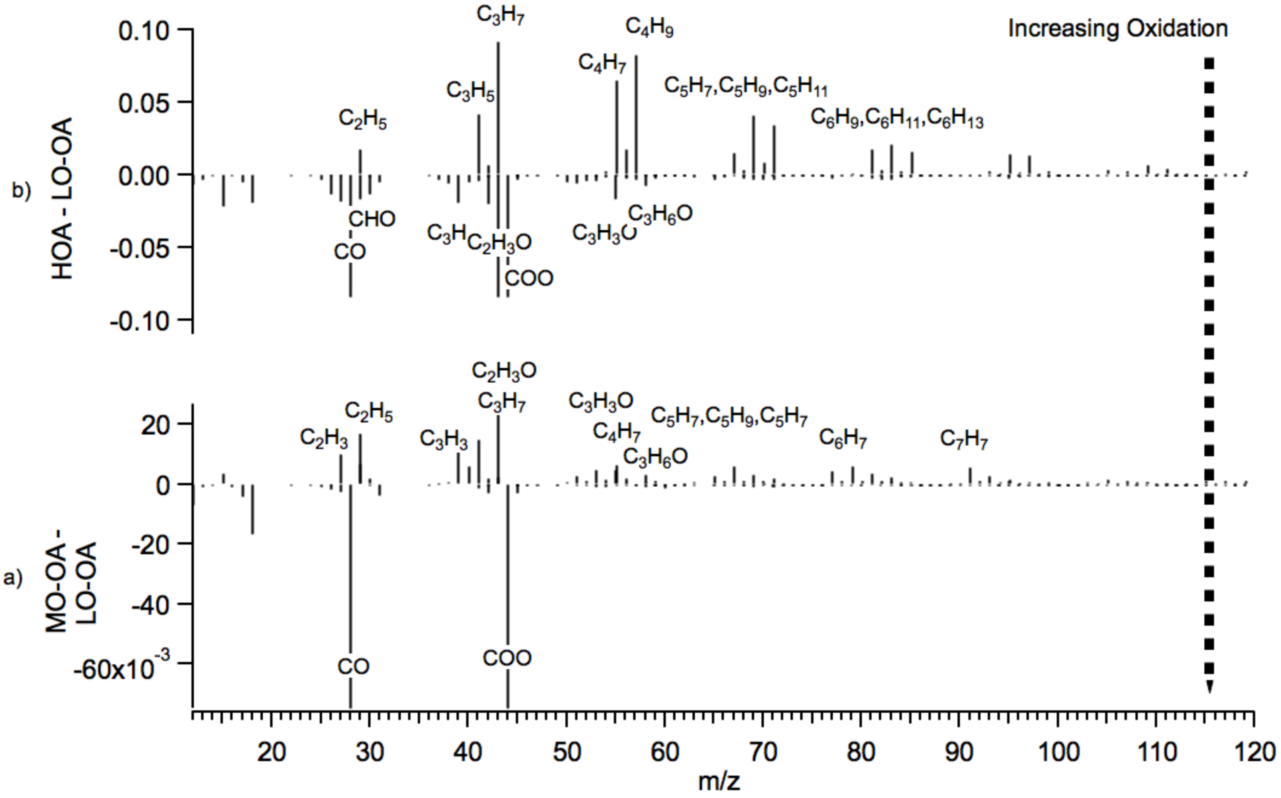

Figure S10 shows the normalized difference between HOA and LO-OA (panel a) and LO-OA and MO-OA (panel b). A relative reduction in the higher-mass hydrocarbon fragments and an increase in the oxidized organic fragments are observed between HOA and LO-OA. This difference spectrum is similar to that found by Sun et al., (2012) between spectra obtained just prior to and during peaks in traffic (when the spectra would be mostly comprised of HOA). The main difference between LO-OA and MO-OA was the level of oxidation; the *m/z* 44 and 28 (COO^+ and CO^+, respectively) increased in MO-OA while the rest of fragments decreased in relative concentration.

2. Aerosol Size-Resolved Chemical Composition

Both pToF AMS and SMPS data show that the prominent particle mode was significantly smaller during periods of heavy traffic than during periods of low traffic influence. In the afternoon, and particularly during periods with increased concentration of SOA, the SMPS number-weighted geometric mode diameter rose (Figure 3D). To study the chemical differences between particles of different sizes, the size-resolved aerosol mass spectra was probed. The calculation of the HR-ToF-AMS spectra for five different size bins revealed that organic aerosol dominated the lowest (50-90 nm) size range while sulfate and nitrate contributed more significantly to the larger (greater than 165 nm) aerosol particles (Figure 7). The size-resolved concentrations of *m/z* 57 ($C_4H_9^+$) and 44 (COO^+) were also examined and found to have opposite correlations with size: the POA hydrocarbon tracer peak (*m/z* 57) dominated the aerosol spectra in the small sizes, while the aged, oxidized organic aerosol tracer peak (*m/z* 44) dominated the larger sizes (Figure 7, Figure S3).

Thus, traffic emissions greatly influenced the number concentration of aerosol, and most of the traffic aerosol was comprised of hydrocarbons. However, oxidized organic species and inorganic species dominated the overall mass concentration of aerosol due to their larger size. Both the HR-ToF-AMS and SMPS size distributions during high- and low-traffic periods measured in this field campaign agreed with previous findings that direct traffic particulate emissions are primarily comprised of small particles (e.g., Sun et al., 2012).

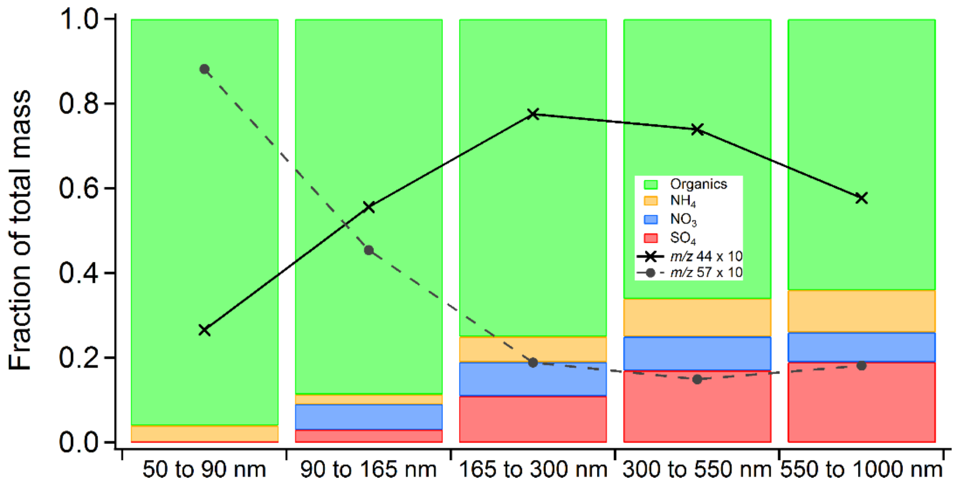

Figure 11: The SO_4, NH_4, NO_3, and organic fraction of total mass for non-refractory submicrometer aerosol particles five different size bins (A, left axis) and the fraction of *m/z* 44 and *m/z* 57, multiplied by 10 .

Figure S12: Comparison of the BC measured by a Multi-Angle Absorption Photometer (MAAP) located in the MASSALYA platform and EC measured by a Sunset Laboratories thermal analyzer located at the Air Rhone Alps station.

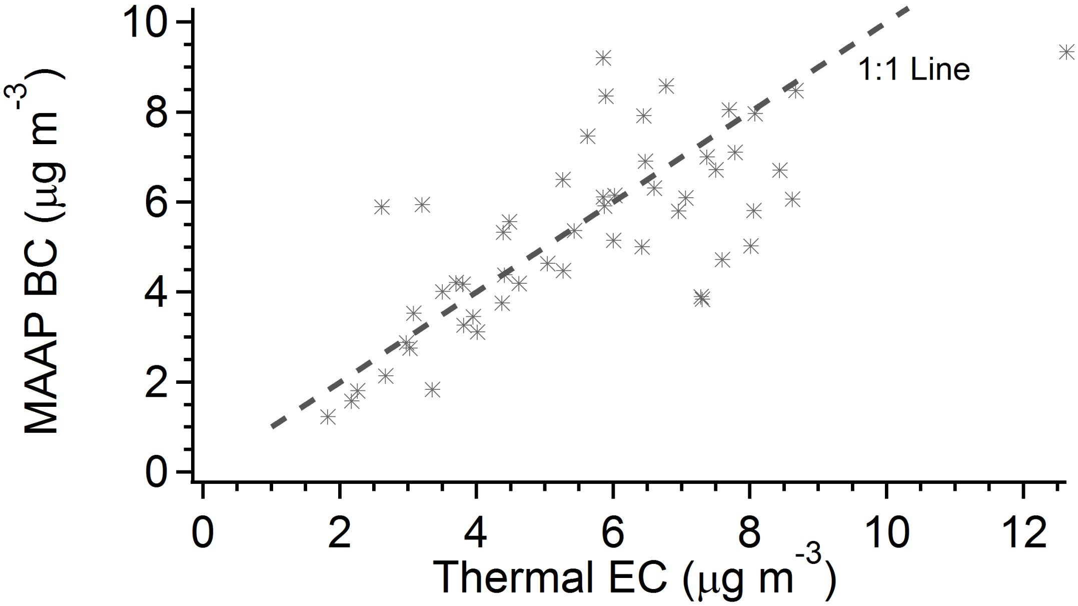

3. NO/NOx/Nitrogen

One possible effect of increased NOx on aerosol formation is the formation of organic nitrate aerosols from the photochemical reactions of various VOC precursors in the presence of high levels of NOx (Ng et al., 2007). During the field campaign, little evidence of typical organic nitrate peaks (e.g., CH_4NO, C_2H_5NO, C_3H_4NO, CH_2NO_3, CH_2NO_2 (Farmer et al., 2010) was found in the high resolution mass spectra. In low concentrations, organic nitrates are difficult to observe in the HR-ToF-AMS as the high energy of ionization (70 eV) used to ionize molecules in the HR-ToF-AMS likely causes most organic nitrate to fragment into organic species and nitrate species in the mass spectra (Farmer et al., 2010). Deviations of the NO_{aero}:NO_{2aero} ratio (*m/z* 30 and *m/z* 46, respectively) from the inorganic nitrate ratio of these two mass fragments in the measured HR-ToF-AMS spectra has been proposed to indicate the presence or absence of organic nitrate (Bruns et al., 2010; Farmer et al., 2010; Fry et al., 2013). Note that, in this paragraph, NO_{aero} and NO_{2aero} refer to peaks in the aerosol mass spectra, not gas-phase NOx. Individual instrument tuning and sensitivity can change the ratio of NO and NO_2; however, the ratio should remain the same throughout a measurement period for inorganic nitrate (Farmer et al., 2010). During the campaign, the aerosol NO_{aero}: NO_{2aero} ratio was about 4.6 when the best-fit line was forced through the origin. This ratio varied throughout the day: from midday to evening, when temperatures and photolysis rates were highest, the bulk aerosol NO_{aero}: NO_{2aero} ratio was greater than 4.6 (Figure 14). This peak in the NO_{aero}: NO_{2aero} ratio corresponded to a daily dip in the aerosol nitrate concentration (although still greater than the limit of detection of 0.06) and to the peak solar hours, which suggests that organic nitrates, if present, were likely both small contributors to the total nitrate measured and also formed from photochemical processing, not directly emitted by vehicles.

In addition, the N-containing peaks within the spectrum of the NOA factor contained mostly amine-like fragments and had a diurnal pattern that was not correlated to changes in the NO_{aero}: NO_{2aero} ratio; thus, the NOA factor resolved was likely not composed of organic nitrates but rather composed of amine-containing organic species. The O: C ratio of the NOA factor was calculated to be 0.4, greater than the 0.07 O: C ratio calculated for the HOA factor spectrum. Russell et al. (2011) identified small but constant concentrations of amines from aerosol measured in a variety of environments and attributed these amines, in part, to combustion processes. Thus, diesel-related emissions could possibly be the source for the observed NOA factor. During the campaign, the calculated NOA factor and measured BC (BC most likely due to diesel emissions) had no significant (R^2=0.09, n=3926) correlation. Thus, while the NOA factor resolved temporally resembled a traffic-related emission, it is not definitively linked to traffic emission tracers. Therefore, its exact source is difficult to determine. Possibly the NOA factor represents the rapid formation of semi-volatile SOA from diesel VOC emissions, but the different lifetimes of VOCs versus aerosol, and the issue of transport and aging for SOA formation, would make this difficult to definitively determine.

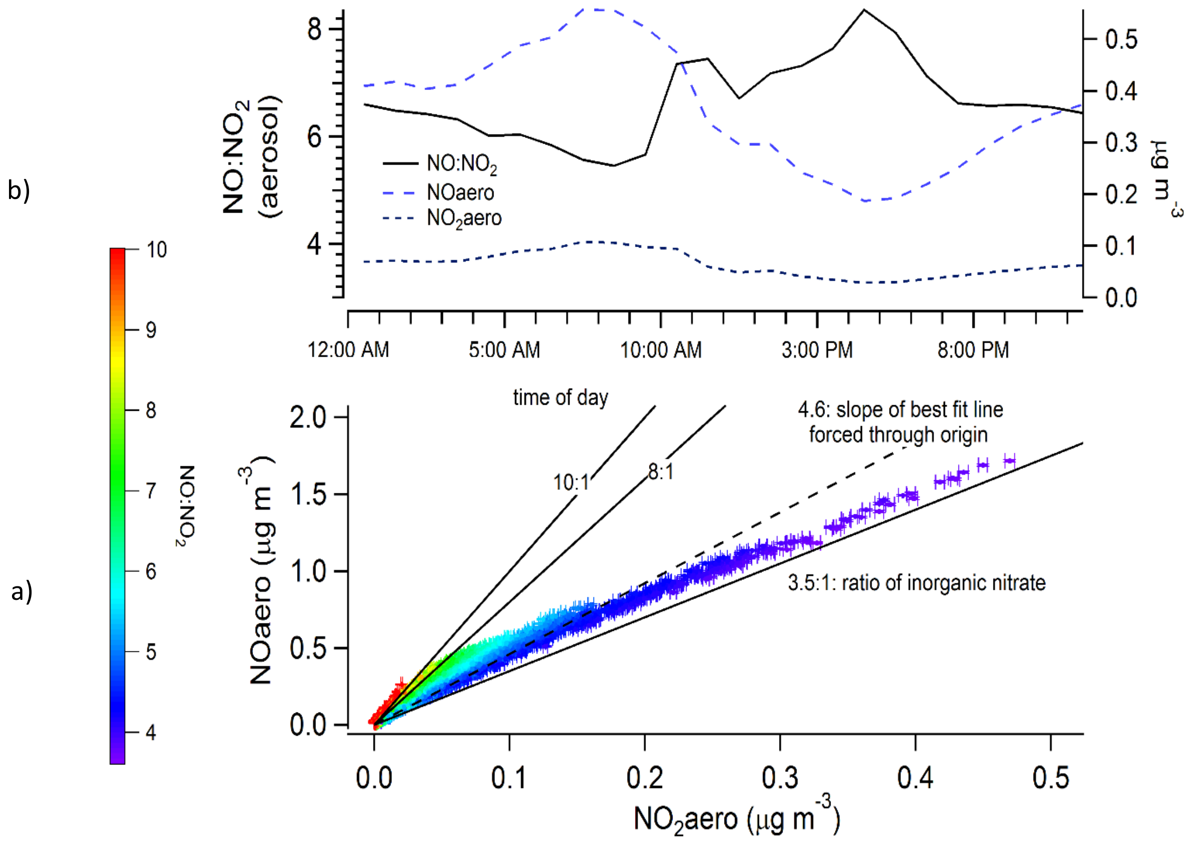

Figure S13: High resolution NO_{aero} and NO_{2aero} peaks from the HR-ToF-AMS-HR-TOF-AMS, colored by the NO: NO_2 ratio (A). NO: NO_2 aerosol ratio diurnal profile (left axis, B) and NO_{aero} and NO2aero HR-ToF-AMS-HR-TOF-AMS diurnal concentrations (right axis, B).